Proceedings of the 270. WE-Heraeus Seminar on: *"Neutron Stars, Pulsars and Supernova Remnants"*
Physikzentrum Bad Honnef, Germany, Jan. 21-25, 2002, eds. W. Becker, H.Lesch & J. Trümper, MPE Report 278, pp. 54- 57

PSR B1951+32 and PSR J0537-6910 - where are the optical counterparts?

R. F. Butler[1], A. Golden[1], A. Shearer[1] and C. Gouiffes[2]

[1] National University of Ireland, Galway; University Road, Galway, Ireland
[2] CEA/DSM/DAPNIA/Service d'Astrophysique, Saclay, Paris, France

arXiv:astro-ph/0208534v2 9 Sep 2002

Abstract. There remain several definitive γ-ray pulsars that are as yet undetected in the optical regime. A classic case is the pulsar PSR B1951+32, associated with the complex CTB 80 SNR. Previous ground based high speed 2-d optical studies have ruled out candidates to $m_V \sim 24$. Hester (2000) has reported an analysis of archival HST/WFPC2 observations of the CTB 80 complex which suggest a compact synchrotron nebula coincident with the pulsar's radio position. Performing a similar analysis, we have identified a possible optical counterpart within this synchrotron nebula at $m_V \sim 25.5$, and another optical counterpart candidate nearby at $m_V \sim$24.2.

PSR J0537-6910 is a young (canonical age $\approx$ 5000 years), 16ms pulsar in the LMC. We report a search for optical pulsations from the region around the X-ray position. We see no obvious candidate exhibiting optical pulsations at the X-ray period, with a 3σ upper limit of $m_V \approx$23.6. We have also examined recent Chandra results (Wang et al. 2001) and show that their X-ray-Optical astrometry is in error by about 7".

1. Introduction

The detection of non-thermal high energy magnetospheric emission from isolated pulsars has remained a non-trivial problem, despite great advances in instrumentation and technological expertise. To date, only 7 optical pulsars have been detected with emission believed to be magnetopsherically dominated, and despite considerable effort, only 8 γ-ray pulsars. In contrast to radio emission, which is generally believed to be generated in close proximity to the magnetic poles, no clear theoretical model construct exists as regards the higher energies. The two principal schools of thought place γ-ray emission localized either to the magnetic poles (Daugherty & Harding 1996) or located further out in the magnetosphere (Romani 1996). Considerable problems remain with these two frameworks, in terms of predicted fluxes, spectral indices and light curve morphologies, and it is clear that further work is required on this subject. This is all the more relevant when one attempts to address the growing empirical database of lower energy emission, in particular in the optical regime. A consequence of non-linear processes within the magnetosphere, this synchrotron emission forms a useful constraint with which one can attempt to comprehensively develop a self-consistent theoretical framework.

2. PSR B1951+32

The pulsar PSR B1951+32, located within the complex combination supernova remnant (SNR) CTB 80, was first identified as a steep-spectrum, point-like source in the radio (Strom 1987), and discovery of radio pulses with an unusually fast 39.5-s period quickly followed (Kulkarni et al. 1988). Canonically, the pulsar's age and the estimated dynamical age of the SNR are consistent at $\sim 10^5$ yrs (Koo et al. 1990) and both have been determined to be at a distance of $\sim$ 2.5 kpc. There is thus general agreement that the association is valid. Evidence for pulsed emission was subsequently found in gamma-rays (Ramanamurthy et al. 1995) and possibly in X-rays (Safi-Harb et al. 1995; Chang & Ho 1997). The ROSAT observations in the X-ray regime do indicate a complex light curve strongly dominated by the intense X-ray radiation of a pulsar-powered synchrotron nebula (Safi-Harb et al. 1995; Becker & Truemper 1996). The unambiguous double-peaked γ-ray (EGRET) light curve obtained by Ramanamurthy et al. (1995) at the appropriate spin-down ephemeris suggested that the pulsar had a conversion efficiency, in terms of rotational energy to γ-rays, of ~ 0.004. Consequently there are strong grounds for the possibility of an optical detection. Using a ground-based MAMA detector in the TRIFFID camera, we have previously examined the central field of CTB 80, but could find no evidence of pulsations in either B or V from this region (O'Sullivan et al., 1998).

2.1. Analysis of archival HST/WFPC2 observations

We obtained from the HST archive all existing WFPC2 data of the CTB 80 SNR, as listed in Table 1. The core of the CTB 80 remnant lies on chip WF3 of the WFPC2 camera in every case. Image processing and photometry were performed using the IRAF (Tody 1993), STSDAS,

Table 1. List of WFPC2 observations of the CTB 80 SNR, obtained from the ST-ECF HST archive.

Date	*Filter*	*TotalExptime*	*Notes*
2/10/97	*F656N*	5300	*HII*
2/10/97	*F673N*	5400	*SII*
2/10/97	*F502N*	5400	*OIII*
2/10/97	*F547M*	2600	Strömgreny

Table 2. The positions and magnitudes derived by DAOPHOT-II/allstar PSF-fitting for point sources detected in the WFPC2 F547M image of CTB 80. The "Dist." column contains the distance from from each source to the centre of the synchrotron nebula; only sources within 5.0" of this position are listed here.

#	*RA*(2000) *hh* : *mm* : *ss.ss*	*Dec*(2000) *dd* : *mm* : *ss.s*	*Dist.* *arcsec*	MAG_{F547M} *magnitudes*
1_{HST}	19 : 52 : 58.24	32 : 52 : 41.0	0.20	23.93 ± 0.30
2_{HST}	19 : 52 : 58.25	32 : 52 : 41.8	0.97	22.15 ± 0.07
3_{HST}	19 : 52 : 58.23	32 : 52 : 42.0	1.11	21.35 ± 0.07
4_{HST}	19 : 52 : 58.28	32 : 52 : 39.9	1.16	24.21 ± 0.12
5_{HST}	19 : 52 : 58.14	32 : 52 : 39.0	2.23	24.07 ± 0.12
6_{HST}	19 : 52 : 58.14	32 : 52 : 43.4	2.69	21.84 ± 0.07
7_{HST}	19 : 52 : 58.42	32 : 52 : 39.2	2.90	21.61 ± 0.06
8_{HST}	19 : 52 : 58.39	32 : 52 : 38.7	2.95	21.96 ± 0.07
9_{HST}	19 : 52 : 58.48	32 : 52 : 42.6	3.55	23.00 ± 0.09
10_{HST}	19 : 52 : 57.95	32 : 52 : 40.8	3.57	25.73 ± 0.26
11_{HST}	19 : 52 : 58.39	32 : 52 : 44.1	3.73	24.25 ± 0.14
12_{HST}	19 : 52 : 57.97	32 : 52 : 39.1	3.79	25.87 ± 0.47
13_{HST}	19 : 52 : 58.02	32 : 52 : 37.1	4.68	22.90 ± 0.07
14_{HST}	19 : 52 : 58.38	32 : 52 : 36.6	4.74	24.44 ± 0.18

and DAOPHOT-II (Stetson 1994) packages. The images in each band were stacked and cleaned of cosmic rays and hot pixels using standard techniques. The F547M intermediate-width band enabled us to perform a deep photometric search for faint stellar sources, to S/N=2 at $MAG_{F547M} = 26.7$. More details of our reduction procedure, including refinement of the HST astrometry using the 2MASS point-source catalog, can be found in Butler et al. (2002). The photometric and astrometric results are shown in Figure 1 and Table 2.

The two "best" radio positions for PSR B1951+32, from Foster et al. (1990) [interferometric] and Foster et al. (1994) [glitchless timing], are shown overplotting the HST field and its detected point-source content in Figure 1. Two point-sources were found to be the most positionally consistent with these two radio positions; the first (object 4_{HST} in Table 2) is a straightforward point-source measurement at $MAG_{F547M} = 24.21 \pm 0.12$; whereas the second (object 1_{HST}) is superimposed on the compact

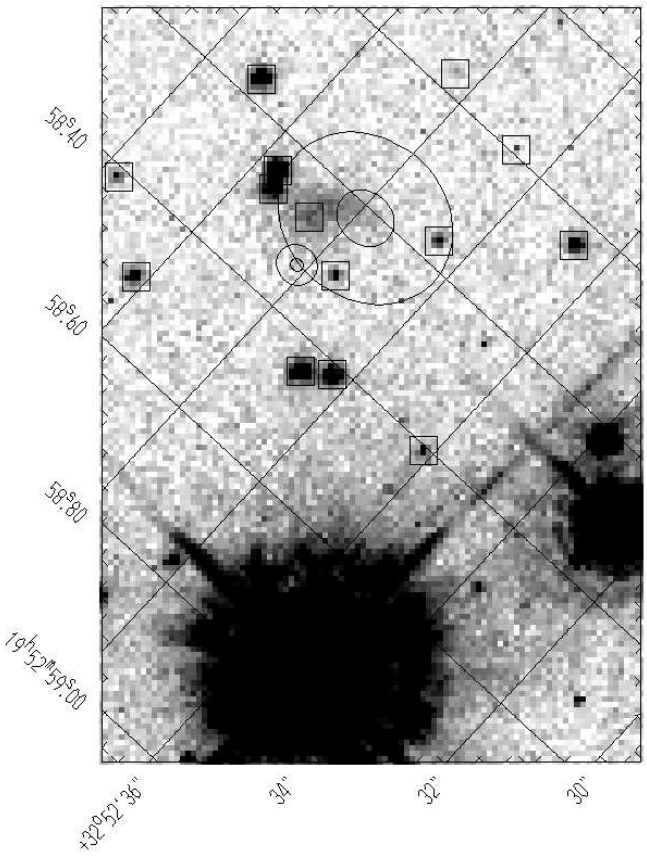

Fig. 1. Section of the HST/WFPC2 F547M image of the core of CTB80. The compact synchrotron nebular knot reported by Hester (2000) can be seen at the upper-centre. The coordinate grid shows our improved astrometric calibration after referencing to the 2MASS point-source catalog. The mapped radio positions for PSR B1951+32 (see text) are marked by black ellipses, the semi-major and semi-minor axes of which are determined by the 1-σ and 3-σ total positional uncertainties in RA and Dec - ie. the quoted error on the radio position, combined with the total rms error on the HST-2MASS fit for 31 stars. The larger pair of ellipses mark the interferometric position. The positions derived by DAOPHOT-II/allstar PSF-fitting for all measured point sources within 5.0" of the centre of the synchrotron nebula are indicated by black squares: counterpart candidate 1_{HST} lies within the nebula and candidate 4_{HST} lies just below it.

synchrotron knot reported by Hester (2000), and required photometric simulations to determine its true magnitude, at MAG_{F547M} between 25.0 - 26.0. Further Monte Carlo simulations to determine the limiting magnitude of the WFPC2 observation showed that an object within this magnitude range is indeed detectable against such nebular background in this data, albeit with S/N of only ≈2 - 2.5.

Crucially, the corrected magnitude of MAG_{F547M} = 25.0 - 26.0 for object 1_{HST} is within the range predicted by the successful mode framework of Pacini & Salvati (1987) and more recently the phenomenological analysis of Shearer & Golden (2001). The magnitude of object 4_{HST} is also consistent with these models, at the brighter end of the predicted range. Consequently, taken together with their positions with respect to the two radio-position error ellipses, we suggest that these two objects are plausible new optical counterpart candidates to PSR B1951+32.

3. PSR J0537-6910

PSR J0537-6910 was first observed by RXTE satellite (Marshall et al. 1998). ROSAT observations by Wang et al. (1998) showed that the pulsar lies within the SNR N157B near the 30 Doradus star formation region in the LMC. The spin period (16 ms) and age ($\approx$ 5000 years) make it the fastest spinning young pulsar known. Scaling the expected optical emission from the Crab pulsar, using the Pacini & Savati (1987) model, we would expect a pulsed magnitude in the range $m_B \approx$ 19-21. Using archival CCD data, both Mignani et al. (2000) and Gouiffes & Ögelman (2001) show no obvious counterpart candidate down to 23rd magnitude.

3.1. TRIFFID Observations

We observed the region around the ROSAT position in February 2000 using the ESO 3.6m telescope and the TRIFFID 2-d photometer. This instrument consists of a relatively low quantum efficiency MAMA detector, observing in B and V, in combination with a high sensitivity (system QE 25 %) group of avalanche photodiodes (APDs). The primary APD was positioned towards the centre of the X-ray error circle on candidate star 16 on Figure 2. Conditions were not photometric and the seeing varied between 1.1" and 1.6". The region was observed on two nights for a total of 5 hours. No pulsed signal was observed from the APD at a limiting magnitude of $m_R \approx 24$. A timing signal was then searched for in the MAMA data, at the locations of all stars marked within the 7"-radius circle in Figure 2; again no signal was seen. A final search was then performed over the full area of the 7"-radius error circle using a set of multiplexed seeing width apertures; again no signal at the pulsar frequency was observed. Our limiting magnitude is estimated as $m_B = 23.6$ at the 3 σ level. This upper limit implies a pulsed optical / X-ray ratio of about 10^{-3}.

3.2. The Chandra-HST registration of the N157B field

We obtained from the HST archive all WFPC2 images which overlapped the field of N157B. The only moderately deep exposures where in the F606W filter ("wide V-band"). Again, image processing, astrometry, and photometry were performed with STSDAS, IRAF, and DAOPHOT-II. We searched for possible pulsar optical counterpart candidates amongst the stars detected within the ROSAT X-ray error circle for PSR J0537-6910, centred at RA 05:37:47.1 Dec -69:10:23.0, by mapping this coordinate into the astrometric solution in the WFPC2 file headers. Figure 3 shows the colour-magnitude diagram for

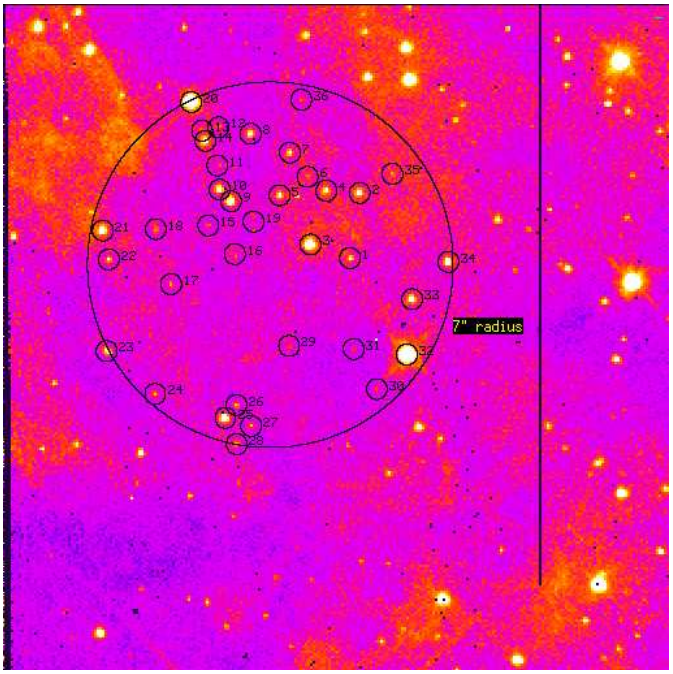

Fig. 2. Section of the HST/WFPC2 F606W image (see Section 4.2) of N157B. This shows the circular region, of 7" radius and centered on the ROSAT position for PSR J0537-6910, which was searched by the TRIFFID photometer.

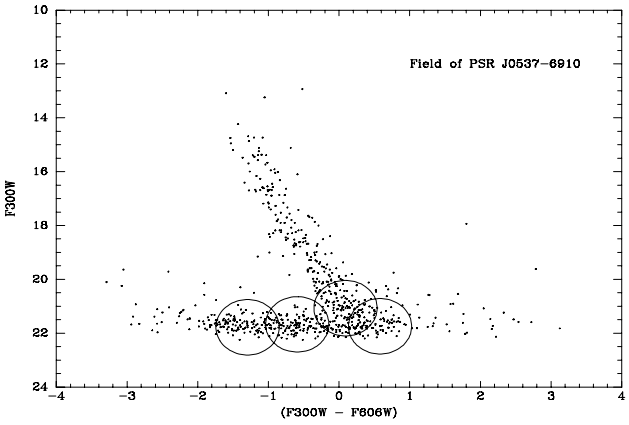

Fig. 3. The HST/WFPC2 colour magnitude diagram (in F300W, F300W-F606W) for stars in the N157B field. Circles mark the stars within the Chandra error circle for PSR J0537-6910 (see Figure 4 below). The bluewards tail at F300W$\approx$22 is an artefact of the different depths in the two filters.

the stars in the field. A similar analysis, using the RA & Dec derived by Wang et al. (2001) for the pulsar in their Chandra observations, yielded a similar optical (mapped) position, albeit with a somewhat smaller error circle. However a comparison with the same analysis by Wang et al. (2001), shown in their Fig. 2, shows a striking positional difference of approx. 7 - 8 arcsec. This is very difficult to explain, as the Chandra coordinate for the pulsar should be good to 1 arcsec, based on agreement of this order with the 2 Wolf-Rayet stars in the X-ray field; and the average absolute pointing error for the HST pipeline astrometric solution (based on the Guide Star Catalog) is 0.8 - 1.5 arcsec (Biretta et al. 2000). Furthermore, our astrometry on the HST image (shown in Figure 4) agrees very well with our independent astrometry on NTT-SUSI imagery (Gouiffes & Ögelman, 2001). One must conclude that some error was made in the Chandra-HST registration of the N157B field by Wang et al. (2001).

Indeed, if the X-ray contours in Fig. 2 of Wang et al. (2001) were shifted to agree with our computed position, then these X-ray contours would match the underlying nebulosity structures much better. This would also have the effect of weakening their argument regarding the extended X-ray emission extending "beyond [filament] F4" - the extent would drop back by about 2 contour levels - although it is not entirely incorrect. More seriously, their statement that "the image shows no evidence for the optical counterpart of the pulsar" surely becomes invalid, as they apparently searched the wrong area of the HST image.

Although we can better address the latter question, having searched the correct area of the HST image, we cannot report a convincing optical counterpart either, because the HST exposures were not deep enough - especially in the F300W filter (approx. U-band), which prevented us from obtaining colour indices (U-V) of the fainter F606W sources. This illustrates the need for deeper, high-resolution imaging and time-resolved imaging. The TRIFFID photometer would be capable of reaching 26th magnitude with 10 hours of observation under reasonable conditions.

Acknowledgements. The authors gratefully acknowledge financial support from Enterprise Ireland under the Basic Research Programme. RFB is also grateful for financial support from the Improving Human Potential programme of the European Commission (contract HPFM-CT-2000-00652). This publication is partly based upon Hubble Space Telescope data obtained from the ST-ECF archive, ESO, Garching, Germany. It also makes use of data products from the Two Micron All Sky Survey, which is a joint project of the University of Massachusetts and the Infrared Processing and Analysis Center/California Institute of Technology, funded by the National Aeronautics and Space Administration and the National Science Foundation. Finally, we also wish to thank Richard Strom for useful suggestions and comments while we prepared this paper.

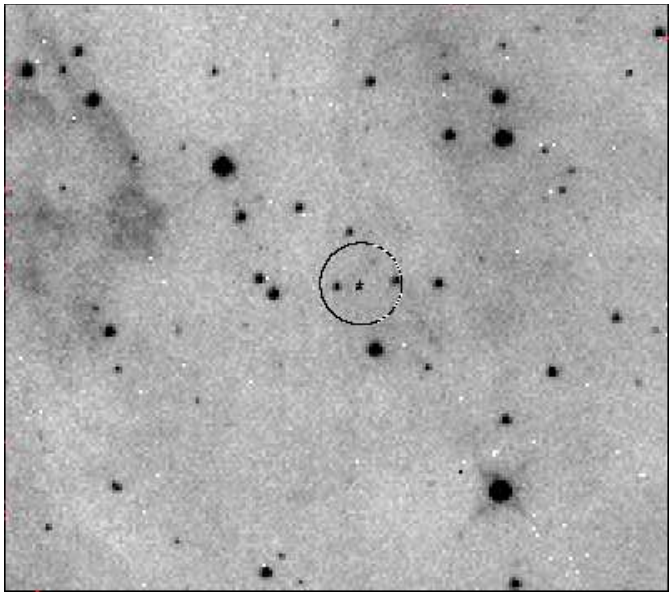

Fig. 4. Aligned HST/WFPC2 field and Chandra X-ray error circle for PSR J0537-6910, from this work.

References

Becker, W., & Trümper, J., 1996, A&AS, 120, 69
Biretta, J. A., et al., 2000, "WFPC2 Instrument Handbook, Version 5.0", (Baltimore: STScI)
Butler, R. F., Golden, A., & Shearer, A., 2002, accepted for publication in A&A
Chang, H.-K., & Ho, C., 1997, ApJ, 479, L125
Daugherty, J.K., & Harding, A. K., 1996, A&AS, 120, 107
Gouiffes, C., & Ögelman, H., 2001, PUAS2000 Conference, ASP 202, 301
Hester J., 2000, AAS, 197, 8216
Koo, B.-C., Reach, W. T., Heiles, C., Fesen, R. A., & Shull, J. M., 1990, ApJ, 364, 178
Kulkarni, S. R., Clifton, T. C., Backer, D. C., Foster, R. S., Fruchter, A. S., 1988, Nature, 331, 50
Marshall, et al., 1998, ApJ, 499, L179
Mignani, R., et al., 2000, A&A, 355,603
O'Sullivan, C., et al., 1998, A&A, 335, 991
Pacini, F., & Salvati, M., 1987, ApJ, 321, 447
Ramanamurthy, P. V., et al., 1995, ApJ, 447, L109
Romani, R. W., 1996, ApJ, 470, 469
Safi-Harb, A., Ögelman, H., & Finley, J. P., 1995, ApJ, 439, 722
Shearer A., & Golden A., 2001, ApJ, 547, 967
Stetson, P. B., 1994, PASP 106, 250
Strom, R. G., 1987, ApJ, 319, L103
Tody, D., 1993, ASP Conf. Ser. 52: Astronomical Data Analysis Software and Systems II, eds. R. J. Hanisch, R. J. V. Brissenden, & J. Barnes, 173
Wang, Q. D. & Gotthelf, E. V., 1998, 509, L109
Wang, Q. D., Gotthelf, E. V., Chu, Y.-H., & Dickel, J. R. 2001, ApJ, 559, 275